Available online at www.sciencedirect.com
SCIENCE DIRECT®
Journal of Electron Spectroscopy and Related Phenomena 144–147 (2005) 1249–1252
JOURNAL OF ELECTRON SPECTROSCOPY and Related Phenomena
www.elsevier.com/locate/elspec

Hole-concentration dependence of electrical resistivity in the (Bi, Pb)$_2$(Sr, La)$_2$CuO$_{6+\delta}$ quantitative evaluation with angle-resolved photoemission spectroscopy

Takeshi Kondo[a,*], Tsunehiro Takeuchi[b], Takayoshi Yokoya[c], Syunsuke Tsuda[c], Shik Shin[c], Uichiro Mizutani[a]

[a] *Department of Crystalline Materials Science, Nagoya University, Furo-cho, Chikusa-ku, Nagoya 464-8603, Japan*
[b] *Ecotopia Science Institute, Nagoya University, Nagoya 464-8603, Japan*
[c] *Institute of Solid State Physics, University of Tokyo, Kashiwa 277-8581, Japan*

Available online 17 March 2005

Abstract

Relaxation time of Bloch states at the Fermi level (τ_F), Fermi velocity (v_F), and mean free path (l_F) of the conduction electrons in the (Bi, Pb)$_2$(Sr, La)$_2$CuO$_{6+\delta}$ (Bi2201) superconductors with various hole-concentration (p) were determined by the angle-resolved photoemission spectroscopy (ARPES) measurement with high energy- and momentum-resolutions; $\Delta E = 10$ meV and $\Delta k = 0.005$ Å^{-1}. We found that τ_F at k_F along (0, 0)–(π, π) cut is kept constant over a wide Hole-concentration range while it in the vicinity of (π, 0) is drastically shortened with decreasing p and eventually reaches nearly zero in the under-doped sample with the transition temperature of 27 K. By calculating electrical resistivity and comparing it with the measured one, we confirmed that τ_F, v_F, and l_F determined by the ARPES measurement can be used for the quantitative estimation of the electrical transport properties, such as the electrical resistivity, in high-T_c cuprates.
© 2005 Elsevier B.V. All rights reserved.

Keywords: ARPES; Electrical resistivity; High-T_c; Cuprate; Bi2201; Superconductor

1. Introduction

Temperature dependence of the electrical resistivity in the CuO_2 plane (*ab*-plane) of the high-T_c cuprates, defined as $\rho_{ab}(T)$, drastically varies with varying hole-concentration (p) [1–4]; the T^2-dependence is observed in $\rho_{ab}(T)$ for the over-doped samples, while the optimally doped sample shows T-linear $\rho_{ab}(T)$ over a wide temperature range up to about 1000 K. In the under-doped samples, $\rho_{ab}(T)$ shows a change in its temperature slope at a temperature (T^*), which gradually increases with decreasing p. This unusual p-dependence in $\rho_{ab}(T)$ would be closely related to the nature of the high-T_c superconducting state. In order to gain deep insight into the origin of high-T_c superconductor, it is, thus, very important to clarify the mechanism that is responsible for these unusual behaviors of $\rho_{ab}(T)$ in high-T_c superconductors.

The band structure (ε–$\boldsymbol{k}$ dispersion) and the relaxation time for Bloch states ($\tau(\boldsymbol{k})$) have to be investigated to quantitatively evaluate the $\rho_{ab}(T)$. Angle-resolved photoemission spectroscopy (ARPES) is a unique and powerful experimental technique because the ε–$\boldsymbol{k}$ dispersion and $\tau(\boldsymbol{k})$ can be deduced from the peak position and the full width of half maximum (FWHM) at the measured spectra, respectively.

We have already obtained the ε–$\boldsymbol{k}$ dispersion in (Bi, Pb)$_2$(Sr, La)$_2$CuO$_{6+\delta}$ (Bi2201) with various p in our previous work [5], where the tight-binding fitting method was carried out for the data sets of electronic energy states ($\varepsilon(k_x, k_y)$) determined by the ARPES measurement. In this study, the momentum dependence of relaxation time of the Bloch states on the Fermi surface, $\tau(\boldsymbol{k}_F)$, was precisely determined from the FWHM of energy distribution curves (EDCs) measured by ARPES. All data was measured at 200 K, where the pseu-

* Corresponding author. Tel.: +81 52 789 4463; fax: +81 52 789 4463.
E-mail address: kondo@mizu.xtal.nagoya-u.ac.jp (T. Kondo).

0368-2048/$ – see front matter © 2005 Elsevier B.V. All rights reserved.
doi:10.1016/j.elspec.2005.01.198

Table 1
Sample preparation conditions for the present Bi2201 single crystals

Nominal composition	Atmosphere	Temperature	T_c (K)	Label
$(Bi_{1.74}Pb_{0.38})Sr_{1.88}CuO_{6+\delta}$	Vacuum	550 °C for 24 h	7	OD7K
$(Bi_{1.35}Pb_{0.85})(Sr_{1.47}La_{0.38})CuO_{6+\delta}$	Ar flow	650 °C for 24 h	35	OP35K
$(Bi_{1.35}Pb_{0.85})(Sr_{1.40}La_{0.45})CuO_{6+\delta}$	Ar flow	650 °C for 24 h	27	UD27K

dogap disappears in all measured samples. By calculating p-dependence of ρ_{ab}(200 K) using the ε–$\boldsymbol{k}$ dispersion and the $\tau(\boldsymbol{k}_F)$ determined in this study, we demonstrate that the high resolution ARPES can be a powerful tool to quantitatively evaluate the electron transport properties.

2. Experimental procedure

(Bi, Pb)$_2$(Sr, La)$_2$CuO$_{6+\delta}$ (Bi2201) single crystals were grown by the conventional floating-zone (FZ) technique. The single synthesized crystals were cut into typically (1–3) mm × 3 mm × 0.05 mm in dimension both for ARPES and resistivity measurements. We partially substitute Pb for Bi, because this substitution is effective in removing the superstructure along the b-axis [6–8], which is often observed in the Bi-based superconductors as the Umklapp bands [9,10] and prevents us from easily analyzing the band structure.

Hole-concentration, p, was controlled by partially substituting La for Sr, and the condition of the subsequent annealing. The nominal compositions, the annealing conditions, and the resulting T_c are listed in Table 1. We labeled the over-doped sample of $T_c = 7$ K, the optimally doped sample of $T_c = 35$ K, and the under-doped sample of $T_c = 27$ K as OD7K, OP35K, and UD27K, respectively.

The ARPES spectra were accumulated using the Scienta SES 2002 hemispherical analyzer with the Gammadata VUV5010 photon source (He Iα) at the Institute of Solid State Physics (ISSP), the University of Tokyo. The angular and energy resolutions employed in this work were 0.15° and 10 meV, respectively.

3. Results and discussion

Fig. 1(a) shows the angle dependence of Fermi velocity $v_F(\theta)$, given by $v_F = \frac{1}{\hbar}\left(\frac{\partial\varepsilon}{\partial k}\right)_{\varepsilon=\mu}$, for OD7K, OP35K, and UD27K, respectively, where θ is defined as that shown in Fig. 1(b). We used the previously determined ε–$\boldsymbol{k}$ dispersion [5] to calculate $v_F(\theta)$. It is obvious that the $v_F(\theta)$ possesses its minimum at $\theta = 0°$ (near $(\pi, 0)$ point) and increases with increasing θ toward $\theta = 45°$. The $v_F(\theta)$ reflects the topology of the band structure; the saddle point existent at $(\pi, 0)$ near μ, where the velocity is reduced. We realized that $v_F(\theta)$ increases with decreasing p regardless of θ. It's tendency is more enhanced around $\theta = 0°$, while $v_F(45°)$ is almost constant over the whole p.

Fig. 2(a)–(c) shows the 200 K energy distribution curves symmetrized about the chemical potential (μ), $I_{sym}(\boldsymbol{k}_F, \varepsilon)$'s, at three different $\boldsymbol{k}_F$'s for UD27K, OP35K, and OD7K, respectively. The operation of the symmetrization method [11–13] is drawn in Fig. 2(d). Symmetrization method has been often employed to determine the Fermi wave vector because it possesses one peak only at $\boldsymbol{k}_F$. We used this method in different ways such that the relaxation time τ is determined. The ARPES spectrum can be expressed as $I(\boldsymbol{k}, \varepsilon) = f(\varepsilon)A(\boldsymbol{k}, \varepsilon)$, where $A(\boldsymbol{k}, \varepsilon)$ and $f(\varepsilon)$ represent one-particle spectral function and Fermi–Dirac distribution function, respectively. $A(\boldsymbol{k}, \varepsilon)$ at $\boldsymbol{k}_F$ has, in general, symmetrical shape centered at μ, and that the condition $A(\boldsymbol{k}_F, \varepsilon) = A(\boldsymbol{k}_F, -\varepsilon)$ is satisfied. If we use the symmetrization method for the measured $I(\boldsymbol{k}_F, \varepsilon)$, the resulting spectrum, shown in Fig. 2(d), turns out to be one-particle spectral function as $I_{sym}(\boldsymbol{k}_F, \varepsilon) = A(\boldsymbol{k}_F, \varepsilon)f(\varepsilon) + A(\boldsymbol{k}_F, -\varepsilon)f(-\varepsilon) = A(\boldsymbol{k}_F, \varepsilon)f(\varepsilon) + A(\boldsymbol{k}_F, \varepsilon)(1 - f(\varepsilon)) = A(\boldsymbol{k}_F, \varepsilon)$. Indeed, the resulting $A(\boldsymbol{k}_F, \varepsilon)$ possess a single Lorentzian-type shape. It is obvious that the $I_{sym}(\boldsymbol{k}_F, \varepsilon)$ at $\theta = 0°$ is drastically broadened with decreasing p and that the peak

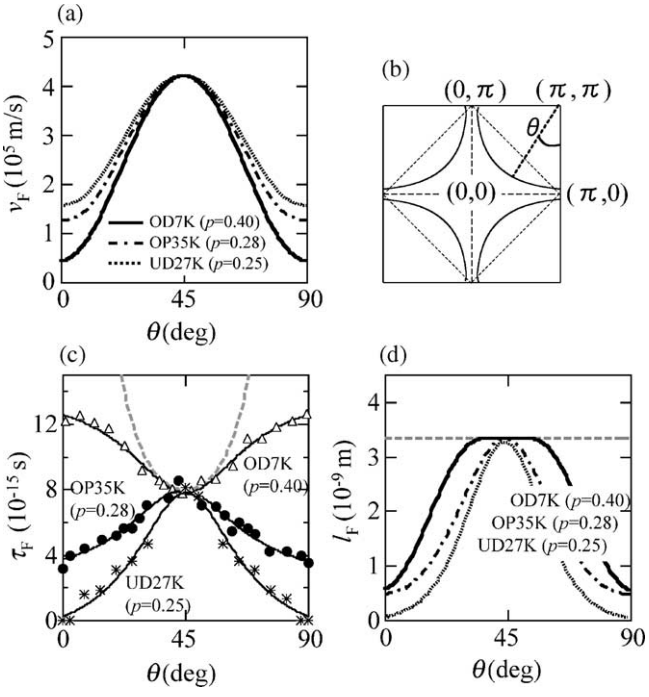

Fig. 1. Relaxation time of Bloch states at the Fermi level (τ_F), Fermi velocity (v_F), and mean free path (l_F) determined by the ARPES measurement. (a) Angle dependence of v_F evaluated by using the ε–$\boldsymbol{k}$ dispersion, where angle is defined as shown in (b). (b) Fermi surface in the first Brillouin zone. Antiferromagnetic zone boundary is shown with dashed lines. (c) Angle dependence of τ_F determined from the FWHM of the ARPES spectra. (d) Angle dependence of l_F calculated by $l_F(\theta) = v_F(\theta)\tau_F(\theta)$.

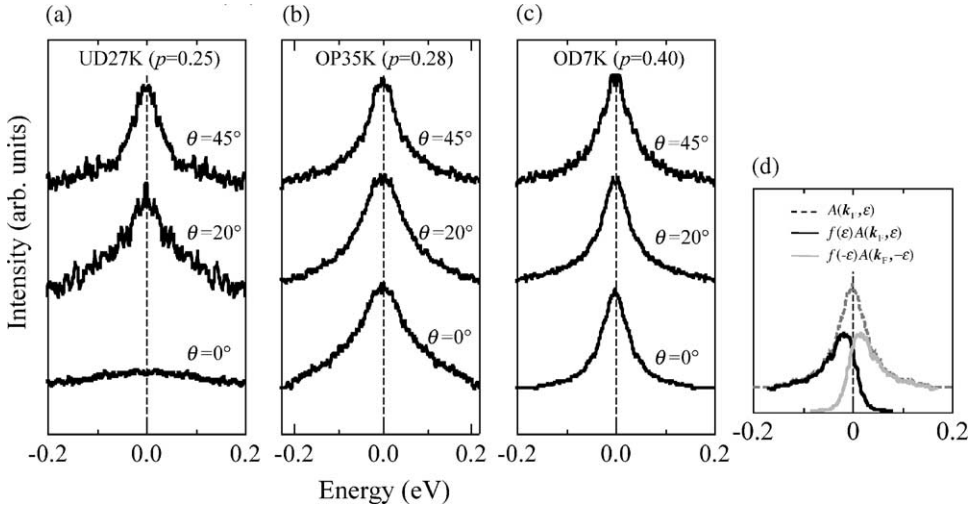

Fig. 2. EDCs at $\boldsymbol{k}_F$ symmetrized about μ for: (a) under-doped sample of $T_c = 27$ K, (b) optimally doped sample of $T_c = 35$ K, and (c) over-doped sample of $T_c = 7$ K. (d) ARPES spectra of $f(\varepsilon)A(\boldsymbol{k}_F, \varepsilon)$, $f(\varepsilon)A(\boldsymbol{k}_F, -\varepsilon)$, and resulting $A(\boldsymbol{k}_F, \varepsilon)$.

is completely disappeared for UD27K, while the $I_{sym}(\boldsymbol{k}_F, \varepsilon)$ at $\theta = 45^\circ$ shows almost same shape regardless of p.

In Fig. 1(c), we plot τ at $\boldsymbol{k}_F$ as a function of θ, $\tau_F(\theta)$, which is determined from the FWHM of $I_{sym}(\boldsymbol{k}_F, \varepsilon)$ using the relation of $\tau \approx \hbar/\Delta\varepsilon_{FWHM}$. Here, $\Delta\varepsilon_{FWHM}$ is obtained by fitting $I_{sym}(\boldsymbol{k}_F, \varepsilon)$ with a Lorentzian function. We found that $\tau_F(0^\circ)$ is drastically shortened with decreasing p, and eventually reaches zero in UD27K, in sharp contrast with p-independent $\tau_F(45^\circ)$.

The antiferromagnetic (AF) fluctuation should gradually develop with decreasing p because the Mott insulator of AF ordering is stabilized at $p = 0$. This fluctuation behaves as the strong scatterer especially at the antiferromagnetic zone boundary (AFZB), that is corresponding to the momentum line connecting $(0, \pi)$ and $(\pi, 0)$ (see Fig. 1(b)). The broad spectrum, which indicates the presence of the strong scattering, is indeed observed around the $(\pi, 0)$ point, where AFZB contacts with FS of under-doped cuprates superconductors [14,15]. The p dependence of $\tau_F(\theta)$ in Fig. 1(c) indicates that the AF-fluctuation, that would be effective only around $\theta = 0^\circ$, is weaken with increasing θ toward $\theta = 45^\circ$, because $\boldsymbol{k}_F$ moves away from AFZB with increasing θ. One may wonder $\tau(0^\circ)$ should not be longer than $\tau(45^\circ)$ even at the over-doped samples. However, this point can be well accounted for by using mean free path, described below.

Next, we calculated the θ dependence of the mean free path ($l_F(\theta)$) using an equation, $l_F(\theta) = \tau_F(\theta)v_F(\theta)$. Surprisingly, $l_F(\theta)$ for OD7K has a constant value over a wide range of $35^\circ \leq \theta \leq 55^\circ$. Since phonon scattering would cause θ-independent l_F, constant l_F over the wide θ range means that the phonon-scattering determines l_F at this particular θ range. With decreasing p, the $l_F(\theta)$ is drastically decreased especially at $\theta = 0$. The decrease in $l_F(\theta)$ with decreasing p indicates that the some scattering processes are strongly developed. This effect is obvious near $(\pi, 0)$ point, where electrons on the FS no longer contribute electron transport properties. In other words, the effective area of FS become smaller with decreasing p.

Here we calculate the hypothetical $\tau_F(\theta)$ that provides constant l based on phonon-scattering over all θ range. The phonon-based hypothetical $\tau_F(\theta)$ and $l_F(\theta)$, defined as $\tau_F(\theta)_{phonon}$ and $l_F(\theta)_{phonon}$, are shown in Fig. 1(c) and (d) by a dashed line. Notably, the $\tau_F(\theta)_{phonon}$ increases when θ goes away from 45° and the $\tau_F(\theta)_{phonon}$ overlaps $\tau_F(\theta)$ of OD7K at $35^\circ \leq \theta \leq 55^\circ$. This results means that phonon-scattering is dominant in OD7K at $35^\circ \leq \theta \leq 55^\circ$, and that the electron scattering associated with AFZB is already developed in OD7K over the θ range other than $35^\circ \leq \theta \leq 55^\circ$, that can be confirmed by recognizing smaller $\tau_F(\theta)$ of OD7K than $\tau_F(\theta)_{phonon}$.

Finally, the electrical resistivity at 200 K, $\rho_{ab}(200\,K)$, was evaluated by using the FS and the $l_F(\theta)$ determined by ARPES measurement at 200 K with the equation,

$$\sigma = \frac{e^2}{(8\pi^3\hbar)} \int dS_F. \quad (1)$$

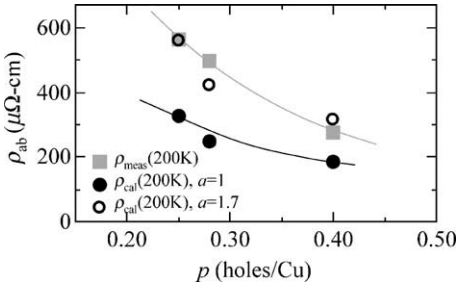

Fig. 3. The calculated electrical resistivity at 200 K, $\rho_{cal}(200\,K)$, by using the FS and l_F determined by the ARPES measurement together with the measured one, $\rho_{meas}(200\,K)$. $\rho_{cal}(200\,K)$ with $a = 1.7$ agrees extremely well with $\rho_{meas}(200\,K)$.

Here the integration is calculated over the whole Fermi surface. The calculated resistivity (ρ_{cal}(200 K)) for OD7K, OP35K, and UD27K are shown with the measured one (ρ_{meas}(200 K)) in Fig. 3 as a function of p, where p was evaluated from the momentum area surrounded by hole-like FS centered at (π, π). The decreasing ρ_{meas}(200 K) with increasing p is qualitatively reproduced by the calculation, though, ρ_{cal}(200 K)'s are still smaller than ρ_{meas}(200 K)'s. Here we noticed that evaluated τ has an ambiguity because it was calculated from the relation $\tau\,\Delta\varepsilon \approx \hbar$. If we use the equation $\tau\,\Delta\varepsilon = \hbar/a$, the resulting resistivity would be a-times larger. We found that the calculated ρ_{cal}(200 K)'s with $a = 1.7$ completely fit the measured one. This result strongly indicates that ARPES can be used for a qualitative evaluation of the electron transport properties such as electrical resistivity.

4. Conclusion

In the present study, we carried out the ARPES measurement on the Bi2201 superconductor with various doping levels at 200 K. The v_F and τ_F were quantitatively determined from the ε–$\boldsymbol{k}$ dispersion and the FWHM of the spectra measured by ARPES, respectively. The drastically decreasing τ_F near $(\pi, 0)$ point with decreasing p indicates that the electron–electron interaction is developed near $(\pi, 0)$. At $\boldsymbol{k}_F$ in the (0, 0)–(π, π) direction, the common l_F is realized regardless of p as a consequence of l_F calculation with $l_F = v_F\tau_F$. The p-independent $l_F(45^\circ)$ and the constant l_F over a wide range of $35^\circ \leq \theta \leq 55^\circ$ in OD7K indicate that the phonon-scattering is dominant around $\boldsymbol{k}_F(45^\circ)$.

We calculated the ρ_{ab}(200 K) by using v_F, τ_F, and FS, and compared it with measured one. The p dependence of ρ_{ab}(200 K) can be quantitatively reproduced by the calculation. We conclude that the ε–$\boldsymbol{k}$ dispersion and τ_F determined by ARPES measurement can be well used for the quantitative estimation of the electrical transport properties, such as the electrical resistivity, in high-T_c cuprates.

References

[1] M. Gurvitch, et al., Phys. Rev. Lett. 59 (1987) 1337.
[2] H. Takagi, et al., Phys. Rev. B 40 (1989) 2254.
[3] S. Martin, et al., Phys. Rev. B 41 (1990) 846.
[4] S. Ono, et al., Phys. Rev. B 67 (2003) 104512.
[5] T. Kondo, et al., J. Electron Spectrosc. Relat. Phenom. 137–140 (2004) 663–668.
[6] Y.-D. Chuang, et al., Phys. Rev. Lett. 83 (1999) 3717.
[7] V. Manivannan, et al., Phys. Rev. B 43 (1991) 8686.
[8] T. Sato, et al., Phys. Rev. B 63 (2001) 132502.
[9] H. Ding, et al., Phys. Rev. Lett. 76 (1996) 1533.
[10] H.M. Fretwell, et al., Phys. Rev. Lett. 84 (2000) 4449.
[11] J. Mesot, et al., Phys. Rev. B 63 (2001) 224516.
[12] T. Takeuchi, et al., J. Electron Spectrosc. Relat. Phenom. 114 (2001) 629.
[13] M.R. Norman, et al., Nature (London) 392 (1998) 157.
[14] Z.-X. Shen, et al., Phys. Rev. Lett. 78 (1997) 1771.
[15] T. Yoshida, et al., Phys. Rev. Lett. 91 (2003) 027001.